

Two Higgs doublets, Effective Interactions and a Strong First-Order Electroweak Phase Transition

Anisha,^{a,b} Lisa Biermann,^c Christoph Englert,^b and Margarete Mühlleitner^c

^a*Department of Physics, Indian Institute of Technology, Kanpur-208016, India*

^b*School of Physics & Astronomy, University of Glasgow, Glasgow G12 8QQ, United Kingdom*

^c*Institute for Theoretical Physics, Karlsruhe Institute of Technology, 76128 Karlsruhe, Germany*

E-mail: anisha@iitk.ac.in, lisa.biermann@kit.edu,
christoph.englert@glasgow.ac.uk, margarete.muehlleitner@kit.edu

ABSTRACT: It is well-known that type II two Higgs doublet models (2HDMs) can struggle to facilitate a strong first-order electroweak phase transition in the early universe whilst remaining theoretically appealing scenarios for many reasons. We analyse this apparent shortfall from the perspective of additional new physics. Starting from a consistent dimension-6 effective field theory Higgs potential extension, we identify the Higgs potential extensions that provide the necessary additional contributions required to achieve a strong first-order electroweak phase transition and trace their phenomenological implications for the Large Hadron Collider. In passing, we critically assess the reliability of the dimension-6 approximation depending on the expected 2HDM phenomenology. In particular, we focus on the role of Higgs pair production (resonant and non-resonant) and interference effects expected in top final states, which are the prime candidates of 2HDM exotics discoveries.

Contents

1	Introduction	1
2	2HDMs and Dimension-6 Higgs Potential Extensions	2
3	Finite Temperature and Phase Transitions	4
3.1	Review of Computational Methods	4
3.2	Scanning Methodology	8
4	Phenomenological Aspects of Effective 2HDM Phase Transitions	9
5	Summary and Conclusions	14

1 Introduction

The null results of searches for new physics beyond the Standard Model (BSM) chiefly performed at the Large Hadron Collider (LHC) have left particle physics in a delicate status quo: The standard paradigms that have shaped BSM model building for the past decades stand challenged, and the role of the TeV scale in nature alongside its microscopic origin are profoundly unclear. This observation is accompanied by insurmountable evidence that new physics is required to reconcile physics at the smallest distances with astrophysical and cosmological observations. The Sakharov criteria [1] provide a strong motivation to incorporate additional sources for CP violation and dynamics responsible for a strong first-order electroweak phase transition to our particle physics picture for efficient baryogenesis. There are various ways to achieve the latter which venture away from minimal SM extensions [2–4]. Nonetheless electroweak baryogenesis remains an attractive avenue and the potential implications for TeV-scale LHC measurements are phenomenologically relevant [5–8].

Along these lines, two Higgs doublet models (2HDMs) remain attractive theories; they have seen continued scrutiny in the literature [9–18]. On the one hand, currently available experimental results are not sensitive enough to move exotic scalar bosons beyond the kinematic reach of the LHC [19]. On the other hand, electroweak precision constraints are avoided similar as in the Standard Model.¹ One important shortfall of 2HDMs, in particular in its type II manifestation that provides a tangible link to supersymmetric UV completions of the SM, is the generic difficulty of obtaining a strong first-order electroweak phase transition (EWPT) for existing parameter constraints [15, 17, 21, 22]. As 2HDM

¹It should be noted that the observed tension in the Kaon sector [17] and the recently experimentally hardened $(g - 2)_\mu$ observation [17, 20] remain difficult to explain in the minimal implementations of the 2HDM.

O_6^{111111}	$(\Phi_1^\dagger \Phi_1)^3$	O_6^{222222}	$(\Phi_2^\dagger \Phi_2)^3$
O_6^{111122}	$(\Phi_1^\dagger \Phi_1)^2 (\Phi_2^\dagger \Phi_2)$	O_6^{112222}	$(\Phi_1^\dagger \Phi_1) (\Phi_2^\dagger \Phi_2)^2$
O_6^{122111}	$(\Phi_1^\dagger \Phi_2) (\Phi_2^\dagger \Phi_1) (\Phi_1^\dagger \Phi_1)$	O_6^{122122}	$(\Phi_1^\dagger \Phi_2) (\Phi_2^\dagger \Phi_1) (\Phi_2^\dagger \Phi_2)$
O_6^{121211}	$(\Phi_1^\dagger \Phi_2)^2 (\Phi_1^\dagger \Phi_1) + \text{h.c.}$	O_6^{121222}	$(\Phi_1^\dagger \Phi_2)^2 (\Phi_2^\dagger \Phi_2) + \text{h.c.}$

Table 1. Dimension-6 operators of class Φ^6 involving Φ_1 and Φ_2 .

dynamics alone do not seem to be quite enough to furnish a strong first-order EWPT, it is the purpose of this paper to clarify the extra dynamics that are required for the 2HDM to provide a sufficiently large EWPT for electroweak baryogenesis. Concretely, we approach this by means of effective field theory (see also [23–25]) and focus in this work on extensions of the scalar potential of the softly broken \mathbb{Z}_2 -symmetric and CP-conserving 2HDM as a well-motivated sector to facilitate a strong first-order EWPT [26–31]. We will focus on the 2HDM type II in this work, but as we will focus mostly on the implications for multi-Higgs production and phenomenological prospects for multi-top final states, our findings generalise to the 2HDM type I straightforwardly.

We organise this work as follows: In Sec. 2 we review the basics of the 2HDM alongside the effective field theory (EFT) modifications we consider in this work. Section 3 provides a short overview of our computational methods. Section 4 is devoted to our results: we provide scans of operators to achieve a strong first-order EWPT and clarify the correlated phenomenological implications relevant for the LHC in multi-Higgs and multi-top final states. We summarise and conclude in Sec. 5.

2 2HDMs and Dimension-6 Higgs Potential Extensions

The tree-level dimension-4 potential of the 2HDM is given by [32, 33]

$$\begin{aligned}
V_{\text{tree}}(\Phi_1, \Phi_2) = & m_{11}^2 (\Phi_1^\dagger \Phi_1) + m_{22}^2 (\Phi_2^\dagger \Phi_2) - m_{12}^2 (\Phi_1^\dagger \Phi_2 + \Phi_2^\dagger \Phi_1) + \lambda_1 (\Phi_1^\dagger \Phi_1)^2 + \lambda_2 (\Phi_2^\dagger \Phi_2)^2 \\
& + \lambda_3 (\Phi_1^\dagger \Phi_1) (\Phi_2^\dagger \Phi_2) + \lambda_4 (\Phi_1^\dagger \Phi_2) (\Phi_2^\dagger \Phi_1) + \frac{1}{2} \lambda_5 [(\Phi_1^\dagger \Phi_2)^2 + (\Phi_2^\dagger \Phi_1)^2] \\
& + \left(\lambda_6 (\Phi_1^\dagger \Phi_1) + \lambda_7 (\Phi_2^\dagger \Phi_2) \right) \left(\Phi_1^\dagger \Phi_2 + \Phi_2^\dagger \Phi_1 \right) \quad (2.1)
\end{aligned}$$

where $\Phi_{1,2}$ are $SU(2)_L$ doublets with hypercharge $Y = 1$. The absence of tree-level flavour-changing neutral interactions can be guaranteed by imposing a \mathbb{Z}_2 symmetry [34], which is softly broken by the term proportional m_{12}^2 . In the following, we will assume only such soft breaking and choose the couplings $\lambda_{6,7} = 0$, which induces a hard breaking of \mathbb{Z}_2 , to be zero. We furthermore take the values of the remaining coupling and mass parameters, λ_i ($i = 1, \dots, 5$) and m_{ab}^2 ($a, b = 1, 2$), to be real.

Including higher-dimensional EFT contributions to the Higgs potential leads to the operators of Tab. 1. The Φ^6 operators² that we focus on in this first investigation give rise to a dimension-6 extension of the 2HDM potential [36–39]

$$\mathcal{L}_{\text{EFT}} = \mathcal{L}_{\text{2HDM}} + \sum_i \frac{C_6^i}{\Lambda^2} O_6^i \quad \Rightarrow \quad V_{\text{dim-6}} = - \sum_i \frac{C_6^i}{\Lambda^2} O_6^i. \quad (2.2)$$

Here, O_6^i are the dimension-6 operators given in Tab. 1 and C_6^i are the corresponding Wilson Coefficients (WCs). As in the unperturbed 2HDM we can solve the tadpole equations to relate m_{11}^2 and m_{22}^2 to the remaining potential parameters in the vacuum. Diagonalisation of the charged and CP-odd Higgs mass mixing matrices is described by the characteristic angle

$$\tan \beta = \frac{v_2}{v_1}, \quad (2.3)$$

which means that even in the presence of our Φ^6 interactions $\tan \beta$ is directly linked to the ratio of vacuum expectation values, while $(246 \text{ GeV})^2 \approx v^2 = v_1^2 + v_2^2$ is fixed by the W boson mass (or equivalently the Fermi constant). Explicit expressions for the masses of the neutral and charged Higgs bosons can be obtained similar as in [36], however, it is convenient for us to choose masses and mixing angles as input parameters. Taking inspiration from the on-shell renormalisation scheme introduced in [15], we perform shifts of the renormalisable part of the Lagrangian, $\lambda_i \rightarrow \lambda_i + \delta\lambda_i$ and $m_{12}^2 \rightarrow m_{12}^2 + \delta m_{12}^2$, with

$$\begin{aligned} \delta\lambda_1^{\text{d6}} &= \frac{1}{4\Lambda^2 v_1^2} [6C_6^{111111} v_1^4 + (2C_6^{121211} + C_6^{122111}) v_1^2 v_2^2 \\ &\quad - \{2(C_6^{112222} + C_6^{121222}) + C_6^{122122}\} v_2^4], \\ \delta\lambda_2^{\text{d6}} &= -\frac{1}{4\Lambda^2 v_2^2} [\{2(C_6^{111122} + C_6^{121211}) + C_6^{122111}\} v_1^4 \\ &\quad - (2C_6^{121222} + C_6^{122122}) v_1^2 v_2^2 - 6C_6^{222222} v_2^4], \\ \delta\lambda_4^{\text{d6}} &= \frac{v_1^2}{\Lambda^2} (C_6^{111122} + C_6^{121211} + C_6^{122111}) \\ &\quad + \frac{v_2^2}{\Lambda^2} (C_6^{112222} + C_6^{121222} + C_6^{122122}), \\ \delta\lambda_5^{\text{d6}} &= \frac{1}{2\Lambda^2} [(2C_6^{111122} + 4C_6^{121211} + C_6^{122111}) v_1^2 \\ &\quad + (2C_6^{112222} + 4C_6^{121222} + C_6^{122122}) v_2^2], \\ \delta m_{12}^{2\text{d6}} &= \frac{v_1 v_2}{2\Lambda^2} [\{2(C_6^{111122} + C_6^{121211}) + C_6^{122111}\} v_1^2 \\ &\quad + \{2(C_6^{112222} + C_6^{121222}) + C_6^{122122}\} v_2^2]. \end{aligned} \quad (2.4)$$

They directly yield mass eigenvalues and mixing angles as in the $d = 4$ 2HDM.³ In the following, we will refer to h and H as the lighter and the heavier CP-even Higgs boson, respectively. A denotes the CP-odd scalar and H^\pm is the charged scalar degree of freedom.

²The dimension-6 operators are classified following the Warsaw basis convention [35].

³A similar consistent choice could be obtained by a different subset of the potential parameters in the dimension-4 Lagrangian.

Model	I	II
ξ_h^u	$\cos \alpha / \sin \beta$	$\cos \alpha / \sin \beta$
ξ_h^d	$\cos \alpha / \sin \beta$	$-\sin \alpha / \cos \beta$
ξ_H^u	$\sin \alpha / \sin \beta$	$\sin \alpha / \sin \beta$
ξ_H^d	$\sin \alpha / \sin \beta$	$\cos \alpha / \cos \beta$
ξ_A^u	$\cot \beta$	$\cot \beta$
ξ_A^d	$\cot \beta$	$-\tan \beta$

Table 2. Coupling modifiers ξ for 2HDM type I and II and up- and down-type quarks relevant for this study.

This means that for any choice of Wilson coefficients we obtain the same mass spectrum and neutral mixing angle in the vacuum as for Eq. (2.1). Any direct coupling of the Higgs bosons to SM matter is therefore insensitive to the Wilson coefficients and the choice of Eq. (2.4) shifts correlations into Higgs self-couplings and multi-Higgs final states, given single Higgs measurements as the transparent input that is typically provided by experimental collaborations and checked for in parameter scans with BSM tools such as **ScannerS** [40–42], **HiggsBounds** [43–46], or **HiggsSignals** [47, 48].⁴

Consequently, the usual classification of the 2HDM according to the \mathbb{Z}_2 assignments applies to this work as well. The Higgs boson couplings to fermions f in the mass basis are given by

$$\mathcal{L}_{\text{Yuk}} = - \sum_{f=u,d,\ell} \frac{m_f}{v} \left(\xi_h^f \bar{f} f h + \xi_H^f \bar{f} f H - i \xi_A^f \bar{f} \gamma_5 f A \right) - \left[\frac{\sqrt{2} V_{ud}}{v} \bar{u} \left(m_d \xi_A^d P_R - m_u \xi_A^u P_L \right) d H^+ + \frac{\sqrt{2}}{v} m_\ell \xi_A^l (\bar{\nu} P_R \ell) H^+ + \text{h.c.} \right], \quad (2.5)$$

where $P_{L,R}$ are the left and right chirality projectors and the coupling modifiers ξ are given in Tab. 2.

3 Finite Temperature and Phase Transitions

In order to calculate the strength of the EWPT in our model, we determine the global minimum of the one-loop corrected effective potential at finite temperature. The derivation of the effective potential is reviewed in Sec. 3.1, our scan is described in Sec. 3.2.

3.1 Review of Computational Methods

The effective potential describes the exact vacuum state [49] of a theory including finite temperature effects [50–52]. It can be derived through a perturbative expansion of the

⁴The dimension-4 parameters can then be obtained by inverting $\delta\lambda_i, \delta m_{12}^2$ in the Λ^{-1} expansion.

generating functional of one-particle irreducible Green's functions. Consequently, the one-loop contribution includes the inverse propagator, independent of the structure of the underlying Lagrangian. In terms of the static field configurations described by $\vec{\omega}$, and the temperature T , the one-loop contribution to the effective potential at finite temperature has the general form

$$V_{\text{eff}}^{(1)}(\vec{\omega}, T) = \sum_{X=S,G,F} (-1)^{2s_X} (1 + 2s_X) I^X, \quad (3.1)$$

with scalar (S), gauge-boson (G) and fermion (F) contributions that have the following form

$$I^S = \frac{T}{2} \sum_n^{\text{Bos}} \int \frac{d^3k}{(2\pi)^3} \sum_i \left[\log \det \left(-\mathcal{D}_{S,i}^{-1} \right) \right], \quad (3.2a)$$

$$I^G = \frac{T}{2} \sum_n^{\text{Bos}} \int \frac{d^3k}{(2\pi)^3} \sum_i \left[\log \det \left(-\mathcal{D}_{GB,i}^{-1} \right) \right], \quad (3.2b)$$

$$I^F = -T \sum_n^{\text{Ferm}} \int \frac{d^3k}{(2\pi)^3} \sum_i \left[\log \det \left(-\mathcal{D}_{F,i}^{-1} \right) \right], \quad (3.2c)$$

with inverse propagators \mathcal{D}^{-1} calculated in finite temperature field theory. Within the imaginary time formalism, the propagators receive temperature-dependent corrections, *e.g.* the inverse scalar propagator in momentum space has the form $\mathcal{D}_S^{-1} = \omega_n^2 + \omega_k^2$ in terms of the discrete Matsubara modes

$$\omega_n^2 = (2n\pi T)^2, \quad n \in \mathbb{N}_0 \quad (3.3)$$

and

$$\omega_k^2 = \mathbf{k}^2 + m^2, \quad (3.4)$$

where in the case of Eq. (3.4), the mass term receives corrections from the EFT operators. At $T = 0$ this gives rise to the vacuum expectation value $v \simeq 246$ GeV as described above.

The integrals in Eq. (3.2) split into a UV-divergent temperature-independent part and a UV-finite, but IR-divergent temperature-dependent part. In the $\overline{\text{MS}}$ -scheme, the one-loop contributions read

$$I_{\overline{\text{MS}}}^X = \underbrace{\frac{m_X^4}{64\pi^2} \left[\log \left(\frac{m_X^2}{\mu^2} \right) - k_X \right]}_{\equiv V_{\text{CW}}(\vec{\omega})} + \underbrace{\frac{T^4}{2\pi^2} J_{\pm} \left(\frac{m_X^2}{T^2} \right)}_{\equiv V_T(\vec{\omega}, T)} \quad (3.5)$$

with $X = \{(S), (G), (F)\}$ and the renormalisation constant k_X

$$k_X = \begin{cases} \frac{5}{6}, & \text{for gauge bosons} \\ \frac{3}{2}, & \text{otherwise} \end{cases} \quad (3.6)$$

and the *thermal* fermionic (+) and bosonic (−) function J_{\pm} [50, 52, 53]

$$J_{\pm}(x^2) = \int_0^{\infty} dk k^2 \log \left(1 \pm e^{-\sqrt{k^2+x^2}} \right). \quad (3.7)$$

The bosonic Matsubara zero modes, $n = 0$, lead to IR divergences that are cancelled by resumming the thermal masses Π [51, 53–57]. The scalar thermal masses are calculated as thermal scalar self-energy corrections in the soft-momentum limit,

$$\begin{aligned} \Pi_{ij}^{(1)}(\mathbf{p} \rightarrow 0, \omega_n \rightarrow 0) &\equiv \Pi_{ij}^{(1)}(0) \\ &= \sum_k \kappa_{ij}^k T \sum_n \int \frac{d^3 p}{(2\pi)^3} \mathcal{D}_{kk}(\omega_n, \omega_p) \\ &\quad + \sum_{k,l} \kappa_{ij}^{kl} T^2 \sum_{n,m} \int \frac{d^3 p_1}{(2\pi)^3} \mathcal{D}_{kk}(\omega_n, \omega_{p_1}) \int \frac{d^3 p_2}{(2\pi)^3} \mathcal{D}_{ll}(\omega_m, \omega_{p_2}). \end{aligned} \quad (3.8)$$

Here, quartic scalar couplings are labelled with κ_{ij}^k , while couplings between six scalars are encoded in κ_{ij}^{kl} . Note, that the latter is already a two-loop correction to the scalar self-energy. The finite temperature field theory integral is evaluated in the high-temperature limit $m/T \ll 1$ as

$$\begin{aligned} T \sum_n \int \frac{d^3 p}{(2\pi)^3} \mathcal{D}_{ij}(\omega_n, \omega_p) &= T \sum_n \int \frac{d^3 p}{(2\pi)^3} \frac{1}{\omega_n^2 + \omega_p^2} \\ &= T \sum_n \int \frac{d^3 p}{(2\pi)^3} \frac{1}{\omega_n^2 + \mathbf{p}^2 + m^2} \simeq T \sum_n \int \frac{d^3 p}{(2\pi)^3} \frac{1}{\omega_n^2 + \mathbf{p}^2} = \dots = \frac{T^2}{12} \left[1 + \mathcal{O}\left(\frac{m}{T}\right) \right]. \end{aligned} \quad (3.9)$$

The dimension-6 operators generate 2-loop contributions $\sim T^4$ (see *e.g.* [28]) which we include throughout our calculation. These derive straightforwardly from the six-point interaction vertices of Tab. 1. Applying the Arnold-Espinosa method [57]⁵, the thermal potential $V_T(\vec{\omega}, T)$ is replaced as

$$V_T(\vec{\omega}, T) \rightarrow V_T(\vec{\omega}, T) + V_{\text{daisy}}(\vec{\omega}, T), \quad (3.10)$$

where

$$V_{\text{daisy}}(\vec{\omega}, T) = -\frac{T}{12\pi} \left[\sum_{i=1}^{n_{\text{Higgs}}} \left((\bar{m}_i^2)^{3/2} - (m_i^2)^{3/2} \right) + \sum_a^{n_{\text{gauge}}} \left((\bar{m}_a^2)^{3/2} - (m_a^2)^{3/2} \right) \right], \quad (3.11)$$

with n_{Higgs} denoting the number of real Higgs fields and n_{gauge} the number of gauge bosons in the adjoint representation of the gauge group. The \bar{m} denote the thermal masses that include the thermal corrections $\Pi^{(1)}$.

As stated above, we introduce shifts to the parameters of the Higgs potential to absorb the effect of the dimension-6 operators such that the masses and mixing angles that we use

⁵For further remarks on this approach and how it compares to the Parwani approach, *cf.* [54, 57]. Further discussions and comparisons are given in [58, 59].

as input parameters remain unchanged. We also require the one-loop corrections to leave the masses and mixing angles at their tree-level values. For this we introduce additional finite counterterms summarised in the counterterm potential V^{CT} and apply the renormalisation conditions

$$0 = \partial_{\phi_i}(V^{\text{CW}} + V^{\text{CT}}|_{\vec{\omega}=\vec{\omega}_{\text{tree}}}) \quad (3.12)$$

$$0 = \partial_{\phi_i} \partial_{\phi_j}(V^{\text{CW}} + V^{\text{CT}}|_{\vec{\omega}=\vec{\omega}_{\text{tree}}}) , \quad (3.13)$$

where ϕ_i denote the scalar Higgs doublet fields developing a non-zero VEV $\bar{\omega}_i$, with $\bar{\omega}_{\text{tree},i}$ being the corresponding tree-level VEV. Note, that for the construction of our counterterm potential, we choose the free parameters arising in the derivation of the potential, *cf.* [15], such that the dimension-6 terms do not introduce new coupling structures. The dimension-6 operator contributions enter through the partial derivatives of V_{CW} which, however, are modified w.r.t. the 2HDM through the dimension-6 contributions to the mass terms. Note, that the dimension-6 operators do not introduce additional new counterterm structures in the above two conditions. For further details on the renormalisation procedure, we refer to [60, 61].

With the dimension-6 extended tree-level potential $V_{\text{tree,dim-6}}$,

$$V_{\text{tree,dim-6}} \equiv V_{\text{tree}} + V_{\text{dim-6}} \quad (3.14)$$

in terms of the tree-level potential V_{tree} of Eq. (2.1) and the dimension-6 potential $V_{\text{dim-6}}$ of Eq. (2.2), we hence have for the loop-corrected effective potential at finite temperature as function of the classical field configuration $\vec{\omega}$,

$$V(\vec{\omega}, T) = V_{\text{tree,dim-6}}(\vec{\omega}) + V_{\text{CW}}(\vec{\omega}) + V_{\text{CT}}(\vec{\omega}) + V_T(\vec{\omega}, T) , \quad (3.15)$$

which we have implemented in the C++ code **BSMPT** [60, 61].

For an electroweak phase transition to be of strong first order, the ratio of the critical VEV v_c at the critical temperature T_c has to fulfil the (conventionally chosen) criterion $\xi_c \equiv v_c/T_c > 1$ to avoid too large baryon washout. The critical temperature is defined as the temperature where there exist two degenerate global minima, one at $v = 0$ and the other at the critical VEV $v_c \neq 0$. The values of T_c , v_c and hence ξ_c are obtained from **BSMPT** which computes the vacuum expectation value $v(T)$ at a given temperature T through the minimisation of the effective potential $V(\vec{\omega}, T)$. The value v is obtained as

$$v(T) = \left(\sum_{k=1}^{n_H} \bar{\omega}_k^2 \right)^{\frac{1}{2}} , \quad (3.16)$$

where n_H means that the sum is performed over all field directions in which we allow for the development of a non-zero electroweak VEV, which are given by the fields that couple to the electroweak gauge bosons. The $\bar{\omega}_k$ denote the field configurations that minimise the loop-corrected effective potential $V(\vec{\omega}, T)$.

3.2 Scanning Methodology

For our numerical analysis, we use parameter points that are compatible with all relevant theoretical and experimental constraints. We resort here to a parameter sample that has been generated recently for the 2HDM [62]. The scan was performed with the help of the program **ScannerS** [40–42]. **ScannerS** chooses as scan parameters the masses of the 2HDM Higgs bosons, $\tan\beta$, the soft breaking mass term m_{12}^2 and the coupling c_{HVV} of the heavier Higgs boson to massive gauge bosons $V \equiv W^\pm, Z$ (instead of the mixing angle α that diagonalizes the neutral CP-even mass matrix). We performed an additional scan to select parameter points with significant branching ratios $\text{BR}(H \rightarrow hh)$ of H into a pair of lighter Higgs bosons h . The total scan ranges of the two merged parameter samples are listed in Tab. 3 for the scenario where the lighter of the two neutral CP-even Higgs bosons, h , takes the role of the SM-like Higgs, denoted as H_{SM} in the following.⁶ We restrict ourselves to the type I and II models. **ScannerS** checks for the theoretical constraints, requiring that the potential is bounded from below, that perturbative unitarity holds and that the electroweak vacuum is the global minimum. For the latter it uses the discriminant from [63].

On the experimental side, we impose compatibility with the electroweak precision data and demand the computed S , T and U values to be within 2σ of the SM fit [64], taking into account the full correlation among the three parameters. One of the neutral CP-even Higgs bosons, in our study chosen to be h , is required to have a mass of [65]

$$m_{H_{\text{SM}}} = 125.09 \text{ GeV} , \quad (3.17)$$

and to behave SM-like. **ScannerS** checks for compatibility with the Higgs signal data through the link to **HiggsSignals** version 2.6.1 [47]. Scenarios with interfering Higgs signals are excluded by forcing the non-SM-like Higgs bosons to lie outside an interval of 5 GeV around 125 GeV in order to avoid interference effects that require a dedicated thorough study beyond the focus of this work. We require 95% C.L. exclusion limits on non-observed scalar states by using **HiggsBounds** version 5.9.0 [43–46]. The sample is also checked with respect to the recent ATLAS analyses in the ZZ [66] and $\gamma\gamma$ [67] final states that were not yet included in **HiggsBounds**. Flavour constraints are taken into account by testing for compatibility with \mathcal{R}_b [68, 69] and $B \rightarrow X_s \gamma$ [69–74] in the $m_{H^\pm} - \tan\beta$ plane. We imposed in the 2HDM type II the latest bound on the charged Higgs mass given in [74], $m_{H^\pm} \geq 800 \text{ GeV}$, for essentially all values of $\tan\beta$. In the type I models, this bound is much weaker and is strongly correlated with $\tan\beta$.

m_h [GeV]	m_H [GeV]	m_A [GeV]	m_{H^\pm} [GeV]	$\tan\beta$	c_{HVV}	m_{12}^2 [GeV ²]
2HDM I/II (light)						
125.09	130...3000	30...3000	85/800...3000	0.8...30	-0.3...1.0	$10^{-5} \dots 10^7$

Table 3. Scan ranges of the 2HDM input parameters, where light refers to the set-up where the lighter of the two CP-even neutral Higgs bosons is the SM-like Higgs H_{SM} , *i.e.* $h \equiv H_{\text{SM}}$.

⁶While also scenarios with $H \equiv H_{\text{SM}}$ still comply with all applied constraints, the plots shown in the following have $h \equiv H_{\text{SM}}$.

The inclusion of the Wilson coefficients in the 2HDM potential modifies the 2HDM mass values and mixing angles. By applying the shifts given in Eqs. (2.4) we ensure, however, that they remain unchanged also after inclusion of the dimension-6 contributions. This allows us to use the **ScannerS** sample of parameter points and work with parameter sets that are compatible with all relevant theoretical and experimental constraints. In practice, we apply within **BSMPT** on the parameters $\lambda_{1,2,4,5}$ and m_{12}^2 of the respective **ScannerS** sample point the shifts of Eqs. (2.4). The values of m_{11}^2 and m_{22}^2 are obtained from the minimisation conditions taking into account the dimension-6 contributions to the Higgs potential. With these parameters and λ_3 for the given parameter point under investigation, **BSMPT** then computes the EWPT for the 2HDM potential including the dimension-6 operators.

4 Phenomenological Aspects of Effective 2HDM Phase Transitions

The general requirements for EFT methods to provide appropriate approximations for momentum-independent Wilson coefficients are twofold. Firstly, the heavy degrees of freedom that are integrated out need to be sufficiently heavy compared to the characteristic energy scale that is probed at the respective laboratory. And secondly, perturbativity, which constitutes the overarching concept of the field-theoretic aspects investigated in this work imposes the additional requirement of dimension-6 terms to be a small correction in relation to the renormalisable dimension-4 result. This provides confidence in neglecting higher order terms in the Λ^{-1} expansion.

The modifications of the 2HDM introduced in Sec. 2 provide a rich landscape for phenomenological deviations. This is particularly interesting for the 2HDM type II that we will mostly focus on in this section. However, as we are mainly considering interactions of the extra Higgs bosons with the top sector, our findings generalise to the 2HDM type I, where a strong first-order electroweak phase transition (SFOEWPT) already at dimension-4 level can be found more easily than in type II.

On the one hand, correlations of masses and couplings are modified away from the dimension-4 expectation when considering effective interactions. On the other hand, such deviations are still allowed to be significant as the LHC has so far only shed limited light on the structure of the Higgs self-interactions. The choice of input parameters enables us to directly choose α^7 , $\tan\beta$ and the Higgs boson masses as relevant input parameters of this study. This has the benefit that electroweak precision constraints and Higgs signal strengths

m_h [GeV]	m_H [GeV]	m_A [GeV]	m_{H^\pm} [GeV]	$\tan\beta$	c_{HVV}	m_{12}^2 [GeV ²]
125.09	681	855	884	1.362	-0.00459	220945

T_c^{d4} [GeV]	$v(T_c)^{\text{d4}}$ [GeV]	ξ_c^{d4}
250.55	226.76	0.91

Table 4. Input parameters of the benchmark point used for Fig. 1.

⁷In terms of c_{HVV} in the **ScannerS** scan.

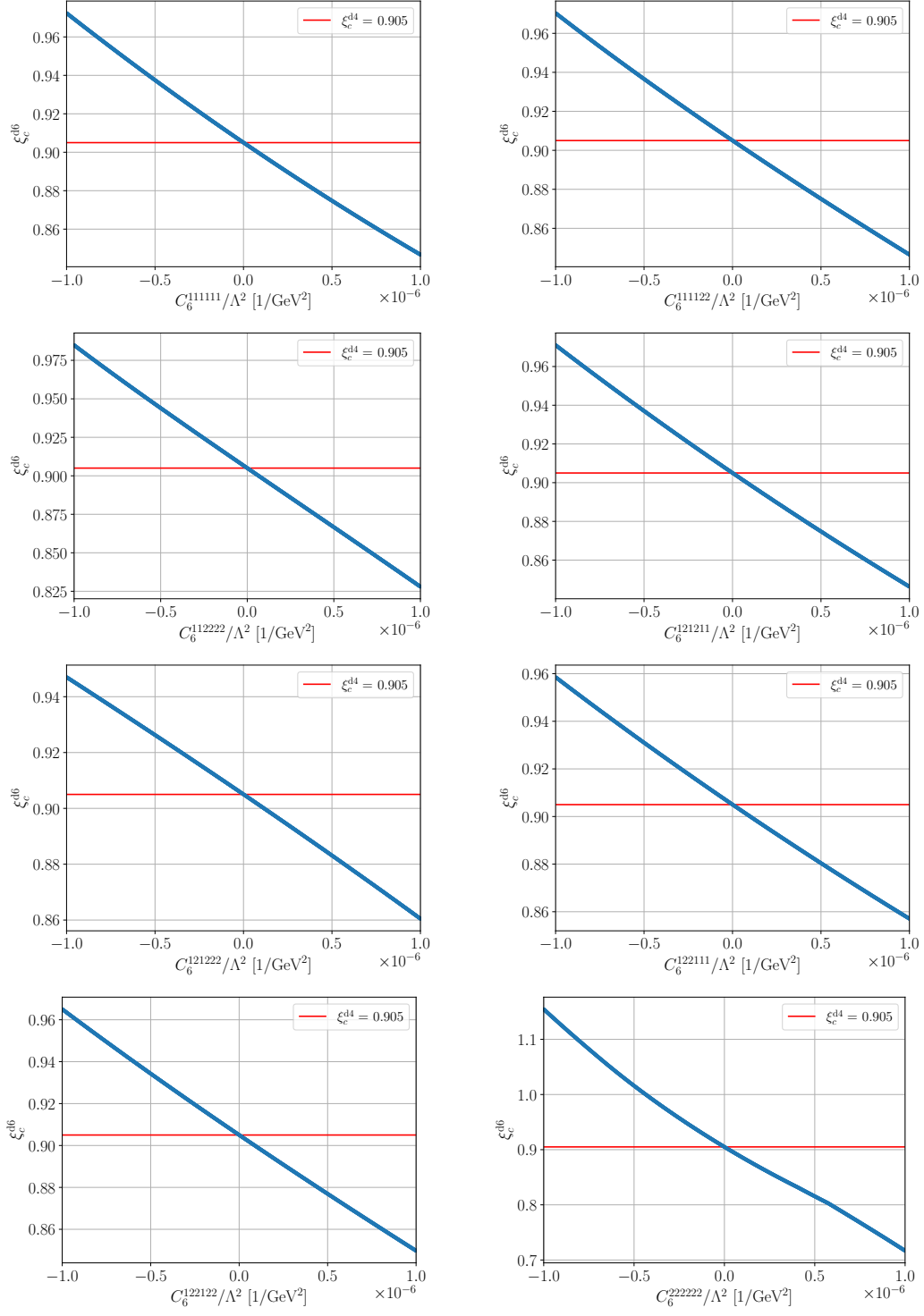


Figure 1. Representative behaviour of ξ_c^{d6} for a representative parameter point of the 2HDM type II of Tab. 4 with $\xi_c^{d4} \simeq 0.9$ when the impact of the individual Wilson coefficients is considered.

are largely unchanged from the dimension-4 result⁸; the modifications of the dimension-6 interactions of Sec. 2 are then primarily visible in modified Higgs self-interactions (*e.g.* Higgs pair production). Consistency of single Higgs collider physics observables with the SM follows closely the usual type I or II paradigms (see [17, 19, 62] for recent analyses).

We first turn to the impact of individual Φ^6 operators of Tab. 1 and how they can contribute to a first-order phase transition.⁹ Reflecting the fact that these additional interactions should be small compared to the dimension-4 theory, in first instance, we consider points that show a relatively strong phase transition $\xi_c^{\text{d4}} \simeq 0.9$ with the measurements as reflected in **HiggsBounds**, **HiggsSignals**, via **ScannerS**. As can be seen in Fig. 1, the effect of additional contributions to the potential creates to good approximation a linear dependence $\sim C_6^i$, which demonstrates the robustness of the approach, *i.e.* the inclusion of non-linear parts in the Λ^{-1} expansion via the Debye masses and the BSMPT approach is numerically insignificant. Furthermore, Fig. 1 clearly shows that an SFOEWPT can be achieved in the 2HDM type II when considering new effective contributions to the Higgs potential at perturbative Wilson coefficient sizes in agreement with current experimental constraints.

The arguably most interesting question then becomes whether the presence of such operators has collider-relevant implications. The latter come in a range of different guises; the phenomenology of the extra Higgs bosons is dominated by top quark final states, in particular when we are relatively close to the alignment limit which is favoured by current collider observations [19]. It is well-known that these are subject to large interference effects that can render the narrow-width approximation unreliable and could even lead to a vanishing direct sensitivity for the naively best-motivated LHC signatures [75] (see also [76–83]). The LHC experiments include these interference effects to their 2HDM searches, *e.g.* [84, 85]. In $gg \rightarrow H \rightarrow t\bar{t}$ the exotic Higgs width is the crucial parameter¹⁰ and it is therefore worthwhile to understand the correlation of ξ_c with the Higgs width feeding into $H \rightarrow t\bar{t}$ searches. Along these lines, the potential lineshape analysis of a future discovery $H \rightarrow t\bar{t}$ could serve as an indirect measurement of the phase transition in the favoured $t\bar{t}$ channel. To this end, we define the interference cross section between gluon fusion $gg \rightarrow H \rightarrow t\bar{t}$ signal and QCD $gg \rightarrow t\bar{t}$ continuum as

$$d\sigma^{\text{inf}} \sim 2\text{Re} \{ \mathcal{M}(gg \rightarrow H \rightarrow t\bar{t}) \mathcal{M}^*(gg \rightarrow t\bar{t}) \} \quad (4.1)$$

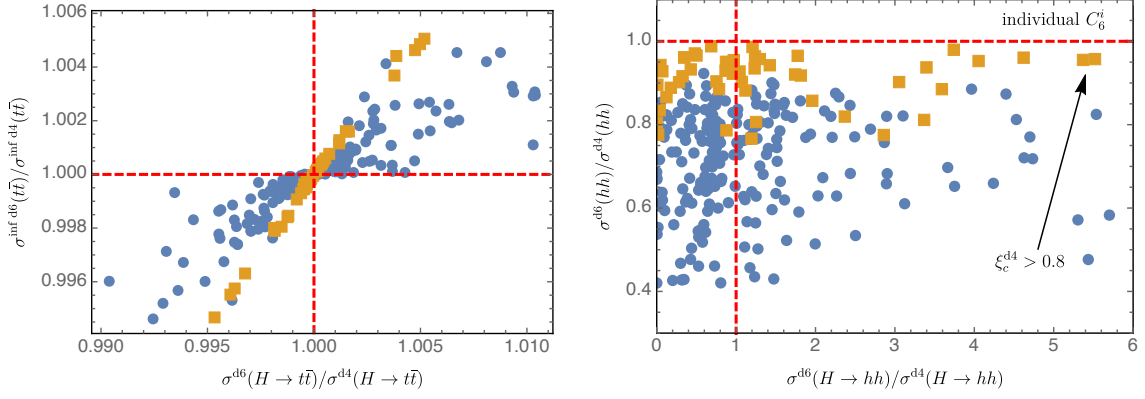
where \mathcal{M} denotes the amplitude (we have suppressed identical phase space and parton density factors and work to leading order accuracy in the following).

In Fig. 2 we show a parameter sample of points in agreement with the constraints described in Sec. 3.2, for $\xi_c^{\text{d4}} > 0.3$ with $\xi_c^{\text{d6}} \simeq 1$ through choices for single Wilson coefficients

⁸We explicitly check that the modified charged Higgs contributions do not impact the SM-like Higgs decay into $\gamma\gamma$.

⁹As stated above, for all results that we present we take parameter scenarios where the lighter of the two CP-even Higgs bosons, h , is the SM-like one.

¹⁰Theoretically this is apparent from the requirement to evaluate the signal component of the process at the complex Higgs pole [86, 87] to guarantee gauge-independence as a consequence of the Nielsen identities [88].



(a) Modification of $gg \rightarrow H \rightarrow t\bar{t}$ and interference effects with continuum $gg \rightarrow t\bar{t}$.

(b) Modification of Higgs pair production $gg \rightarrow hh$ and its correlation with the resonance contribution $gg \rightarrow H \rightarrow hh$.

Figure 2. Correlation between EFT-extended cross sections and their dimension-4 2HDM counterparts. We scan over parameters that are allowed by the constraints detailed in Sec. 3.2, and identify individual Wilson coefficients to achieve $\xi_c^{d6} = 1$. We consider points with $\xi_c^{d4} > 0.3$ and highlight $\xi_c^{d4} > 0.8$ for comparison. For details, see text.

(we will study the effect of combined Wilson coefficients below). We do not distinguish between the individual Wilson coefficients as the phenomenological outcome is qualitatively similar. The scan also includes relatively large Wilson coefficient choices which are necessary to achieve $\xi_c^{d6} \simeq 1$ starting from $\xi_c^{d4} \simeq 0.3$; for illustration purposes we highlight smaller dimension-6 couplings resulting from $\xi_c^{d4} \geq 0.8$ in Fig. 2. The phenomenological baseline of the $d = 4$ points shown in Fig. 2 is a top-philic one; $t\bar{t}$ final states are the preferred decay channels of the exotic Higgs bosons with typically $\text{BR}(H \rightarrow t\bar{t}) \gtrsim 0.8$. The changes that are introduced by the dimension-6 interactions do not (and to be perturbatively robust must not) change this behaviour dramatically. In fact, neither the $t\bar{t}$ final states, nor their width-sensitive interference effects show phenomenologically observable modifications, Fig. 2 (a). There is a trend that reflects the overall ξ_c behaviour, *i.e.* the closer ξ_c^{d4} gets to unity, the smaller the $gg \rightarrow H \rightarrow t\bar{t}$ modification becomes as a result of a smaller modification of the total H decay width. In any case for the generic top-dominated final states, such per mille level effects are well beyond the sensitivity that can be obtained at hadron colliders.

This leaves multi-Higgs final states as motivated signatures as shown in Fig. 2 (b). The resonant $H \rightarrow hh$ contribution is small as $H \rightarrow t\bar{t}$ is preferred, but there can be a modification of the resonance signal $gg \rightarrow H \rightarrow hh$, which is correlated with a modified trilinear Hhh coupling. However, the overall $gg \rightarrow hh$ rate is decreased. For instance we find deviations of 125 GeV Higgs boson pair production of $\sigma^{d6}(hh)/\sigma^{d4}(hh) \simeq 0.4$ (0.8) for $\xi_c^{d4} = 0.3$ (0.9) when sampling individual Wilson coefficient directions. For large distances $1 - \xi_c^{d4}$ it is clear that the EFT contribution needs to overcome the 2HDM contribution alone, which eventually will put pressure on the dimension-6 EFT assumption, highlighted through non-linear dependencies of $\xi_c^{d6}(\{C_6^i\})$. The individual Wilson coefficient scans that we have focussed so far remain in their linear regime and hence robust when viewed

according to this criterion (this quickly changes for correlated Wilson coefficient choices, see below).

The behaviour of the Higgs pair production cross sections in Fig. 2 (b) is mostly due to the fact that additional potential contributions lead to an enhancement of the trilinear SM-like Higgs self-coupling $\sim \lambda_{hhh}$ at the order of $\sim 50\%$. For these coupling deviations the dominant $gg \rightarrow hh$ contribution shows a decreasing behaviour with a rescaling of the light Higgs self-interaction $\kappa_\lambda > 1$ [89–96]. In the light of existing projections of Higgs boson pair production [97, 98] this can be a manageable albeit challenging task at the LHC.¹¹ The analysis of the separated resonant $H \rightarrow hh$ signal in direct comparison to the hh continuum production can therefore serve as an indirect constraint on $\xi_c \sim 1$. Given that discovery of the H state should become possible in $H \rightarrow t\bar{t}$ first, there is significant scope of data-driven methods in separating continuum from on-shell H production.

So far all of our results have been dominated by the general top-philic nature of the exotic Higgs bosons in the 2HDM. Moving to larger dimension-4 couplings in the Higgs sector we can furnish situations where the branching ratio of $H \rightarrow hh$ is significant whilst maintaining reasonable production rates via virtual top quarks. In such an instance the correlation of on-shell production and di-Higgs continuum is less statistically limited and therefore experimentally more feasible. As can be seen in Fig. 3, such parameter points in the 2HDM type II are typically characterised by a larger distance $|1 - \xi_c^{d4}|$. Achieving $\xi_c > 1$ in a controlled way therefore relies on the interplay of different effective operators as can indeed be expected in concrete UV scenarios (*e.g.* in singlet extensions of the scalar sector [22, 30, 100–103]).

In Fig. 4, we show the results of a scan of uniform Wilson coefficients $C_6^i = C$ to achieve $\xi_c^{d6} \simeq 1$, again for $\xi_c^{d4} \geq 0.3$. Furthermore, we also include the Higgs-philic points of Fig. 3 to Fig. 4. These are typically characterised by relatively low ξ_c^{d4} - the price of Higgs-philic H phenomenology. As can be seen, in general our findings are similar to the individual Wilson coefficient scan, with large enhancements possible in the $H \rightarrow hh$ rate. As this starts from a relatively low cross section rate for top-philic H decays, the largest enhancements $\sigma^{d6}(H \rightarrow hh)/\sigma^{d4}(H \rightarrow hh) > 3$ arise from small $H \rightarrow hh$ dimension-4 cross sections. In this instance, a large enhancement is not directly phenomenologically relevant as the cross section still remains small when including $d = 6$ contributions. Yet, enhancements of factors of ~ 2.5 are possible for cross

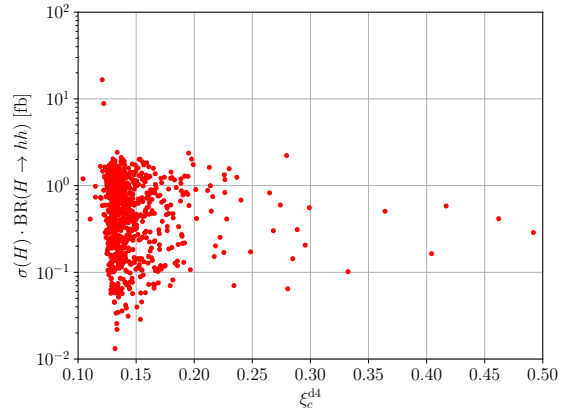


Figure 3. Correlation of the 2HDM value of ξ_c^{d4} and the exotic Higgs production cross section in the double Higgs decay channel.

¹¹The $t\bar{t}hh$ final state showing an increasing cross section for $\kappa_\lambda > 1$ could provide additional sensitivity [99].

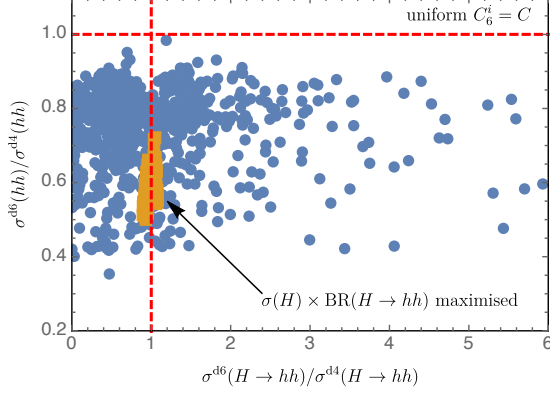


Figure 4. Same as Fig. 2(a) but with uniformly chosen Wilson coefficients $C_6^i = C$ and scanned over C to achieve $\xi_c^{d6} \simeq 1$. We highlight the Higgs-philic scan result points of Fig. 3, which demonstrates that large potential modifications are required to achieve $\xi_c^{d6} \simeq 1$ in this instance, typically starting from $\xi_c^{d4} \simeq 0.15$.

sections in the fb range and we can therefore anticipate some LHC sensitivity here in the $b\bar{b}b\bar{b}$ [104–108] and $b\bar{b}\tau\tau$ channels [92, 109–114]. When turning to points that have a larger $H \rightarrow hh$ probability (highlighted in Fig. 4), the resonance contribution is modified at the 5-10% level, while the continuum receives a 50% modification. We note that for uniform Wilson coefficients squared dimension-6 terms $\sim C_6^i C_6^j / \Lambda^4$ will induce a non-linear behaviour thus highlighting the importance of a full (matching) calculation to obtain more realistic estimates. This is particularly relevant for parameter points with sizeable Higgs-philic branching ratios given in Fig. 3.

5 Summary and Conclusions

A strong first-order phase transition is a cosmological requirement within the context of BSM model building. It proves to be non-trivial as well-motivated SM extensions such as the 2HDM can struggle to produce a sufficiently large strength in the context of electroweak baryogenesis. On the one hand, this could mean that baryogenesis proceeds through mechanisms not associated with the TeV scale. On the other hand, we can understand and address $|1 - \xi_c^{d4}|$ in terms of additional dynamics that facilitate a strong first-order electroweak phase transition as a minimal modification of the TeV scale. We have investigated the latter direction in this work for the 2HDM, which remains a strong contender for a more detailed understanding of the electroweak scale. Reverting to effective field theory techniques for the 2HDM, we consider modifications of the Higgs potential at dimension-6 level for the \mathbb{Z}_2 -symmetric, CP-conserving 2HDM. While the 2HDM type II typically falls short of an SFOEWPT, the distance $|1 - \xi_c^{d4}|$ can be overcome by EFT contributions to the Higgs sector.

Additional dimension-6 dynamics that push the 2HDM over the SFOEWPT finishing line (according to the $\xi_c \simeq 1$ criterion) can then lead to phenomenological consequences for LHC physics. Interference effects of heavy Higgs production in the top final state are width-dependent and therefore sensitive to EFT modifications. The overall effect, however, for the top-philic final states currently preferred by experimental data through the alignment limit renders these effects too small to be measurable at the LHC.

Higgs pair production is an important tool for fingerprinting an SFOEWPT, and the distance $|1 - \xi_c^{d4}|$ is directly correlated with expected Higgs pair production deviation.

Current extrapolations of Higgs pair production to the 3/ab high-luminosity frontier indicate that the LHC should become sensitive enough to partially explore this region (see also the recent [115]), potentially assisted by discoveries in the $t\bar{t}$ channels. For more strongly-coupled Higgs interactions of the renormalisable 2HDM, the $H \rightarrow hh$ signature is more motivated as a signature for 2HDM discovery. In such an instance, the 2HDM type II is not capable of producing an SFOEWPT and a significant modification of the 2HDM Higgs potential is required. While this stretches the reliability of the dimension-6 approximation, there are phenomenologically relevant implications, predominantly the reduction of the $gg \rightarrow hh$ rate and modifications of $gg \rightarrow H \rightarrow hh$. The LHC is capable of exploring both phenomenological arenas to some extent and the discovery of an additional Higgs boson that follows a 2HDM paradigm could therefore be analysed from an SFOEWPT dimension-6 Higgs-EFT angle.

Acknowledgements

We thank Stephan Huber and Jason Veatch for helpful conversations. This work was funded by a Leverhulme Trust Research Project Grant RPG-2021-031. C.E. is supported by the UK Science and Technology Facilities Council (STFC) under grant ST/T000945/1 and the Institute of Particle Physics Phenomenology Associateship Scheme. M.M. is supported by the BMBF-Project 05H21VKCCA.

References

- [1] A. D. Sakharov, *Violation of CP Invariance, C asymmetry, and baryon asymmetry of the universe*, *Pisma Zh. Eksp. Teor. Fiz.* **5** (1967) 32–35.
- [2] I. Affleck and M. Dine, *A New Mechanism for Baryogenesis*, *Nucl. Phys. B* **249** (1985) 361–380.
- [3] J. R. Espinosa, T. Konstandin and F. Riva, *Strong Electroweak Phase Transitions in the Standard Model with a Singlet*, *Nucl. Phys. B* **854** (2012) 592–630, [[1107.5441](#)].
- [4] L. Niemi, M. J. Ramsey-Musolf, T. V. I. Tenkanen and D. J. Weir, *Thermodynamics of a Two-Step Electroweak Phase Transition*, *Phys. Rev. Lett.* **126** (2021) 171802, [[2005.11332](#)].
- [5] L. Niemi, H. H. Patel, M. J. Ramsey-Musolf, T. V. I. Tenkanen and D. J. Weir, *Electroweak phase transition in the real triplet extension of the SM: Dimensional reduction*, *Phys. Rev. D* **100** (2019) 035002, [[1802.10500](#)].
- [6] M. J. Ramsey-Musolf, *The electroweak phase transition: a collider target*, *JHEP* **09** (2020) 179, [[1912.07189](#)].
- [7] O. Gould, J. Kozaczuk, L. Niemi, M. J. Ramsey-Musolf, T. V. I. Tenkanen and D. J. Weir, *Nonperturbative analysis of the gravitational waves from a first-order electroweak phase transition*, *Phys. Rev. D* **100** (2019) 115024, [[1903.11604](#)].
- [8] M. Chala, M. Ramos and M. Spannowsky, *Gravitational wave and collider probes of a triplet Higgs sector with a low cutoff*, *Eur. Phys. J. C* **79** (2019) 156, [[1812.01901](#)].

- [9] G. C. Dorsch, S. J. Huber, K. Mimasu and J. M. No, *Echoes of the Electroweak Phase Transition: Discovering a second Higgs doublet through $A_0 \rightarrow ZH_0$* , *Phys. Rev. Lett.* **113** (2014) 211802, [[1405.5537](#)].
- [10] G. C. Dorsch, S. J. Huber, K. Mimasu and J. M. No, *Hierarchical versus degenerate 2HDM: The LHC run 1 legacy at the onset of run 2*, *Phys. Rev. D* **93** (2016) 115033, [[1601.04545](#)].
- [11] D. Gonçalves, A. Kaladharan and Y. Wu, *Electroweak phase transition in the 2HDM: collider and gravitational wave complementarity*, [2108.05356](#).
- [12] W. Su, A. G. Williams and M. Zhang, *Strong first order electroweak phase transition in 2HDM confronting future Z & Higgs factories*, *JHEP* **04** (2021) 219, [[2011.04540](#)].
- [13] G. C. Dorsch, S. J. Huber, T. Konstandin and J. M. No, *A Second Higgs Doublet in the Early Universe: Baryogenesis and Gravitational Waves*, *JCAP* **05** (2017) 052, [[1611.05874](#)].
- [14] L. Wang, *Inflation, electroweak phase transition, and Higgs searches at the LHC in the two-Higgs-doublet model*, [2105.02143](#).
- [15] P. Basler, M. Krause, M. Muhlleitner, J. Wittbrodt and A. Wlotzka, *Strong First Order Electroweak Phase Transition in the CP-Conserving 2HDM Revisited*, *JHEP* **02** (2017) 121, [[1612.04086](#)].
- [16] G. C. Dorsch, S. J. Huber, K. Mimasu and J. M. No, *The Higgs Vacuum Uplifted: Revisiting the Electroweak Phase Transition with a Second Higgs Doublet*, *JHEP* **12** (2017) 086, [[1705.09186](#)].
- [17] O. Atkinson, M. Black, A. Lenz, A. Rusov and J. Wynne, *Cornering the Two Higgs Doublet Model Type II*, [2107.05650](#).
- [18] P. Basler, M. Mühlleitner and J. Müller, *Electroweak Baryogenesis in the CP-Violating Two-Higgs Doublet Model*, [2108.03580](#).
- [19] O. Atkinson, M. Black, C. Englert, A. Lenz, A. Rusov and J. Wynne, *The Flavourful Present and Future of 2HDMs at the Collider Energy Frontier*, [2202.08807](#).
- [20] P. Athron, C. Balázs, D. H. J. Jacob, W. Kotlarski, D. Stöckinger and H. Stöckinger-Kim, *New physics explanations of a_μ in light of the FNAL muon $g - 2$ measurement*, *JHEP* **09** (2021) 080, [[2104.03691](#)].
- [21] P. Basler, S. Dawson, C. Englert and M. Mühlleitner, *Showcasing HH production: Benchmarks for the LHC and HL-LHC*, *Phys. Rev. D* **99** (2019) 055048, [[1812.03542](#)].
- [22] P. Basler, M. Mühlleitner and J. Müller, *Electroweak Phase Transition in Non-Minimal Higgs Sectors*, *JHEP* **05** (2020) 016, [[1912.10477](#)].
- [23] C. Balazs, G. White and J. Yue, *Effective field theory, electric dipole moments and electroweak baryogenesis*, *JHEP* **03** (2017) 030, [[1612.01270](#)].
- [24] J. de Vries, M. Postma, J. van de Vis and G. White, *Electroweak Baryogenesis and the Standard Model Effective Field Theory*, *JHEP* **01** (2018) 089, [[1710.04061](#)].
- [25] D. Croon, O. Gould, P. Schicho, T. V. I. Tenkanen and G. White, *Theoretical uncertainties for cosmological first-order phase transitions*, *JHEP* **04** (2021) 055, [[2009.10080](#)].
- [26] C. Grojean, G. Servant and J. D. Wells, *First-order electroweak phase transition in the standard model with a low cutoff*, *Phys. Rev. D* **71** (2005) 036001, [[hep-ph/0407019](#)].

- [27] S. W. Ham and S. K. Oh, *Electroweak phase transition in the standard model with a dimension-six Higgs operator at one-loop level*, *Phys. Rev. D* **70** (2004) 093007, [[hep-ph/0408324](#)].
- [28] D. Bodeker, L. Fromme, S. J. Huber and M. Seniuch, *The Baryon asymmetry in the standard model with a low cut-off*, *JHEP* **02** (2005) 026, [[hep-ph/0412366](#)].
- [29] X.-m. Zhang, *Operators analysis for Higgs potential and cosmological bound on Higgs mass*, *Phys. Rev. D* **47** (1993) 3065–3067, [[hep-ph/9301277](#)].
- [30] S. Profumo, M. J. Ramsey-Musolf and G. Shaughnessy, *Singlet Higgs phenomenology and the electroweak phase transition*, *JHEP* **08** (2007) 010, [[0705.2425](#)].
- [31] D. E. Morrissey and M. J. Ramsey-Musolf, *Electroweak baryogenesis*, *New J. Phys.* **14** (2012) 125003, [[1206.2942](#)].
- [32] J. F. Gunion, H. E. Haber, G. L. Kane and S. Dawson, *The Higgs Hunter’s Guide*, vol. 80. Perseus Publishing, 2000.
- [33] J. F. Gunion and H. E. Haber, *The CP conserving two Higgs doublet model: The Approach to the decoupling limit*, *Phys. Rev. D* **67** (2003) 075019, [[hep-ph/0207010](#)].
- [34] S. L. Glashow and S. Weinberg, *Natural Conservation Laws for Neutral Currents*, *Phys. Rev. D* **15** (1977) 1958.
- [35] B. Grzadkowski, M. Iskrzynski, M. Misiak and J. Rosiek, *Dimension-Six Terms in the Standard Model Lagrangian*, *JHEP* **10** (2010) 085, [[1008.4884](#)].
- [36] Anisha, S. Das Bakshi, J. Chakraborty and S. Prakash, *Hilbert Series and Plethystics: Paving the path towards 2HDM- and MLRSM-EFT*, *JHEP* **09** (2019) 035, [[1905.11047](#)].
- [37] A. Crivellin, M. Ghezzi and M. Procura, *Effective Field Theory with Two Higgs Doublets*, *JHEP* **09** (2016) 160, [[1608.00975](#)].
- [38] U. Banerjee, J. Chakraborty, S. Prakash and S. U. Rahaman, *Characters and group invariant polynomials of (super)fields: road to “Lagrangian”*, *Eur. Phys. J. C* **80** (2020) 938, [[2004.12830](#)].
- [39] S. Karmakar and S. Rakshit, *Higher dimensional operators in 2HDM*, *JHEP* **10** (2017) 048, [[1707.00716](#)].
- [40] R. Coimbra, M. O. P. Sampaio and R. Santos, *ScannerS: Constraining the phase diagram of a complex scalar singlet at the LHC*, *Eur. Phys. J. C* **73** (2013) 2428, [[1301.2599](#)].
- [41] R. Costa, R. Guedes, M. O. P. Sampaio and R. Santos, *SCANNERS project*, October, 2014.
- [42] M. Mühlleitner, M. O. P. Sampaio, R. Santos and J. Wittbrodt, *ScannerS: parameter scans in extended scalar sectors*, *Eur. Phys. J. C* **82** (2022) 198, [[2007.02985](#)].
- [43] P. Bechtle, O. Brein, S. Heinemeyer, G. Weiglein and K. E. Williams, *HiggsBounds: Confronting Arbitrary Higgs Sectors with Exclusion Bounds from LEP and the Tevatron*, *Comput. Phys. Commun.* **181** (2010) 138–167, [[0811.4169](#)].
- [44] P. Bechtle, O. Brein, S. Heinemeyer, G. Weiglein and K. E. Williams, *HiggsBounds 2.0.0: Confronting Neutral and Charged Higgs Sector Predictions with Exclusion Bounds from LEP and the Tevatron*, *Comput. Phys. Commun.* **182** (2011) 2605–2631, [[1102.1898](#)].
- [45] P. Bechtle, O. Brein, S. Heinemeyer, O. Stål, T. Stefaniak, G. Weiglein et al., *HiggsBounds – 4: Improved Tests of Extended Higgs Sectors against Exclusion Bounds from LEP, the Tevatron and the LHC*, *Eur. Phys. J. C* **74** (2014) 2693, [[1311.0055](#)].

- [46] P. Bechtle, D. Dercks, S. Heinemeyer, T. Klingl, T. Stefaniak, G. Weiglein et al., *HiggsBounds-5: Testing Higgs Sectors in the LHC 13 TeV Era*, [*Eur. Phys. J. C* **80** \(2020\) 1211](#), [[2006.06007](#)].
- [47] P. Bechtle, S. Heinemeyer, O. Stål, T. Stefaniak and G. Weiglein, *HiggsSignals: Confronting arbitrary Higgs sectors with measurements at the Tevatron and the LHC*, [*Eur. Phys. J. C* **74** \(2014\) 2711](#), [[1305.1933](#)].
- [48] P. Bechtle, S. Heinemeyer, T. Klingl, T. Stefaniak, G. Weiglein and J. Wittbrodt, *HiggsSignals-2: Probing new physics with precision Higgs measurements in the LHC 13 TeV era*, [*Eur. Phys. J. C* **81** \(2021\) 145](#), [[2012.09197](#)].
- [49] S. R. Coleman and E. J. Weinberg, *Radiative Corrections as the Origin of Spontaneous Symmetry Breaking*, [*Phys. Rev. D* **7** \(1973\) 1888–1910](#).
- [50] L. Dolan and R. Jackiw, *Symmetry Behavior at Finite Temperature*, [*Phys. Rev. D* **9** \(1974\) 3320–3341](#).
- [51] M. E. Carrington, *The Effective potential at finite temperature in the Standard Model*, [*Phys. Rev. D* **45** \(1992\) 2933–2944](#).
- [52] M. Quiros, *Finite temperature field theory and phase transitions*, in *ICTP Summer School in High-Energy Physics and Cosmology*, pp. 187–259, 1, 1999. [hep-ph/9901312](#).
- [53] M. Quiros, *Field theory at finite temperature and phase transitions*, [*Helv. Phys. Acta* **67** \(1994\) 451–583](#).
- [54] R. R. Parwani, *Resummation in a hot scalar field theory*, [*Phys. Rev. D* **45** \(1992\) 4695](#), [[hep-ph/9204216](#)].
- [55] P. B. Arnold, *Phase transition temperatures at next-to-leading order*, [*Phys. Rev. D* **46** \(1992\) 2628–2635](#), [[hep-ph/9204228](#)].
- [56] J. I. Kapusta and C. Gale, *Finite-temperature field theory: Principles and applications*. Cambridge Monographs on Mathematical Physics. Cambridge University Press, 2011, [10.1017/CBO9780511535130](#).
- [57] P. B. Arnold and O. Espinosa, *The Effective potential and first order phase transitions: Beyond leading-order*, [*Phys. Rev. D* **47** \(1993\) 3546](#), [[hep-ph/9212235](#)].
- [58] J. M. Cline and P.-A. Lemieux, *Electroweak phase transition in two Higgs doublet models*, [*Phys. Rev. D* **55** \(1997\) 3873–3881](#), [[hep-ph/9609240](#)].
- [59] J. M. Cline, K. Kainulainen and M. Trott, *Electroweak Baryogenesis in Two Higgs Doublet Models and B meson anomalies*, [*JHEP* **11** \(2011\) 089](#), [[1107.3559](#)].
- [60] P. Basler and M. Mühlleitner, *BSMPT (Beyond the Standard Model Phase Transitions): A tool for the electroweak phase transition in extended Higgs sectors*, [*Comput. Phys. Commun.* **237** \(2019\) 62–85](#), [[1803.02846](#)].
- [61] P. Basler, M. Mühlleitner and J. Müller, *BSMPT v2 a tool for the electroweak phase transition and the baryon asymmetry of the universe in extended Higgs Sectors*, [*Comput. Phys. Commun.* **269** \(2021\) 108124](#), [[2007.01725](#)].
- [62] H. Abouabid, A. Arhrib, D. Azevedo, J. E. Falaki, P. M. Ferreira, M. Mühlleitner et al., *Benchmarking Di-Higgs Production in Various Extended Higgs Sector Models*, [2112.12515](#).
- [63] A. Barroso, P. M. Ferreira, I. P. Ivanov and R. Santos, *Metastability bounds on the two Higgs doublet model*, [*JHEP* **06** \(2013\) 045](#), [[1303.5098](#)].

- [64] GFITTER GROUP collaboration, M. Baak, J. Cúth, J. Haller, A. Hoecker, R. Kogler, K. Mönig et al., *The global electroweak fit at NNLO and prospects for the LHC and ILC*, *Eur. Phys. J. C* **74** (2014) 3046, [[1407.3792](#)].
- [65] ATLAS, CMS collaboration, G. Aad et al., *Combined Measurement of the Higgs Boson Mass in pp Collisions at $\sqrt{s} = 7$ and 8 TeV with the ATLAS and CMS Experiments*, *Phys. Rev. Lett.* **114** (2015) 191803, [[1503.07589](#)].
- [66] ATLAS collaboration, G. Aad et al., *Search for heavy resonances decaying into a pair of Z bosons in the $\ell^+\ell^-\ell'^+\ell'^-$ and $\ell^+\ell^-\nu\bar{\nu}$ final states using 139 fb^{-1} of proton–proton collisions at $\sqrt{s} = 13\text{ TeV}$ with the ATLAS detector*, *Eur. Phys. J. C* **81** (2021) 332, [[2009.14791](#)].
- [67] ATLAS collaboration, G. Aad et al., *Search for resonances decaying to photon pairs in 139 fb^{-1} of pp collisions at $\sqrt{s} = 13\text{ TeV}$ with the ATLAS detector*, .
- [68] H. E. Haber and H. E. Logan, *Radiative corrections to the $Z b$ anti- b vertex and constraints on extended Higgs sectors*, *Phys. Rev. D* **62** (2000) 015011, [[hep-ph/9909335](#)].
- [69] O. Deschamps, S. Descotes-Genon, S. Monteil, V. Niess, S. T’Jampens and V. Tisserand, *The Two Higgs Doublet of Type II facing flavour physics data*, *Phys. Rev. D* **82** (2010) 073012, [[0907.5135](#)].
- [70] F. Mahmoudi and O. Stal, *Flavor constraints on the two-Higgs-doublet model with general Yukawa couplings*, *Phys. Rev. D* **81** (2010) 035016, [[0907.1791](#)].
- [71] T. Hermann, M. Misiak and M. Steinhauser, *$\bar{B} \rightarrow X_s \gamma$ in the Two Higgs Doublet Model up to Next-to-Next-to-Leading Order in QCD*, *JHEP* **11** (2012) 036, [[1208.2788](#)].
- [72] M. Misiak et al., *Updated NNLO QCD predictions for the weak radiative B -meson decays*, *Phys. Rev. Lett.* **114** (2015) 221801, [[1503.01789](#)].
- [73] M. Misiak and M. Steinhauser, *Weak radiative decays of the B meson and bounds on M_{H^\pm} in the Two-Higgs-Doublet Model*, *Eur. Phys. J. C* **77** (2017) 201, [[1702.04571](#)].
- [74] M. Misiak, A. Rehman and M. Steinhauser, *Towards $\bar{B} \rightarrow X_s \gamma$ at the NNLO in QCD without interpolation in m_c* , *JHEP* **06** (2020) 175, [[2002.01548](#)].
- [75] P. Basler, S. Dawson, C. Englert and M. Mühlleitner, *Di-Higgs boson peaks and top valleys: Interference effects in Higgs sector extensions*, *Phys. Rev. D* **101** (2020) 015019, [[1909.09987](#)].
- [76] K. J. F. Gaemers and F. Hoogeveen, *Higgs Production and Decay Into Heavy Flavors With the Gluon Fusion Mechanism*, *Phys. Lett. B* **146** (1984) 347–349.
- [77] W. Bernreuther, A. Brandenburg and M. Flesch, *Effects of Higgs sector CP violation in top quark pair production at the LHC*, [hep-ph/9812387](#).
- [78] D. Dicus, A. Stange and S. Willenbrock, *Higgs decay to top quarks at hadron colliders*, *Phys. Lett. B* **333** (1994) 126–131, [[hep-ph/9404359](#)].
- [79] S. Jung, J. Song and Y. W. Yoon, *Dip or nothingness of a Higgs resonance from the interference with a complex phase*, *Phys. Rev. D* **92** (2015) 055009, [[1505.00291](#)].
- [80] R. Frederix and F. Maltoni, *Top pair invariant mass distribution: A Window on new physics*, *JHEP* **01** (2009) 047, [[0712.2355](#)].
- [81] M. Carena and Z. Liu, *Challenges and opportunities for heavy scalar searches in the $t\bar{t}$ channel at the LHC*, *JHEP* **11** (2016) 159, [[1608.07282](#)].

- [82] B. Hespel, F. Maltoni and E. Vryonidou, *Signal background interference effects in heavy scalar production and decay to a top-anti-top pair*, *JHEP* **10** (2016) 016, [[1606.04149](#)].
- [83] A. Djouadi, J. Ellis, A. Popov and J. Quevillon, *Interference effects in $t\bar{t}$ production at the LHC as a window on new physics*, *JHEP* **03** (2019) 119, [[1901.03417](#)].
- [84] ATLAS collaboration, M. Aaboud et al., *Search for Heavy Higgs Bosons A/H Decaying to a Top Quark Pair in pp Collisions at $\sqrt{s} = 8$ TeV with the ATLAS Detector*, *Phys. Rev. Lett.* **119** (2017) 191803, [[1707.06025](#)].
- [85] CMS collaboration, A. M. Sirunyan et al., *Search for heavy Higgs bosons decaying to a top quark pair in proton-proton collisions at $\sqrt{s} = 13$ TeV*, *JHEP* **04** (2020) 171, [[1908.01115](#)].
- [86] G. Passarino, C. Sturm and S. Uccirati, *Higgs Pseudo-Observables, Second Riemann Sheet and All That*, *Nucl. Phys. B* **834** (2010) 77–115, [[1001.3360](#)].
- [87] S. Gorla, G. Passarino and D. Rosco, *The Higgs Boson Lineshape*, *Nucl. Phys. B* **864** (2012) 530–579, [[1112.5517](#)].
- [88] N. K. Nielsen, *On the Gauge Dependence of Spontaneous Symmetry Breaking in Gauge Theories*, *Nucl. Phys. B* **101** (1975) 173–188.
- [89] T. Plehn, M. Spira and P. M. Zerwas, *Pair production of neutral Higgs particles in gluon-gluon collisions*, *Nucl. Phys. B* **479** (1996) 46–64, [[hep-ph/9603205](#)].
- [90] U. Baur, T. Plehn and D. L. Rainwater, *Determining the Higgs Boson Selfcoupling at Hadron Colliders*, *Phys. Rev. D* **67** (2003) 033003, [[hep-ph/0211224](#)].
- [91] U. Baur, T. Plehn and D. L. Rainwater, *Examining the Higgs boson potential at lepton and hadron colliders: A Comparative analysis*, *Phys. Rev. D* **68** (2003) 033001, [[hep-ph/0304015](#)].
- [92] M. J. Dolan, C. Englert and M. Spannowsky, *Higgs self-coupling measurements at the LHC*, *JHEP* **10** (2012) 112, [[1206.5001](#)].
- [93] J. Baglio, A. Djouadi, R. Gröber, M. M. Mühlleitner, J. Quevillon and M. Spira, *The measurement of the Higgs self-coupling at the LHC: theoretical status*, *JHEP* **04** (2013) 151, [[1212.5581](#)].
- [94] M. J. Dolan, C. Englert, N. Greiner and M. Spannowsky, *Further on up the road: $hhjj$ production at the LHC*, *Phys. Rev. Lett.* **112** (2014) 101802, [[1310.1084](#)].
- [95] R. Frederix, S. Frixione, V. Hirschi, F. Maltoni, O. Mattelaer, P. Torrielli et al., *Higgs pair production at the LHC with NLO and parton-shower effects*, *Phys. Lett. B* **732** (2014) 142–149, [[1401.7340](#)].
- [96] LHC HIGGS CROSS SECTION WORKING GROUP collaboration, D. de Florian et al., *Handbook of LHC Higgs Cross Sections: 4. Deciphering the Nature of the Higgs Sector*, [[1610.07922](#)].
- [97] CMS collaboration, A. M. Sirunyan et al., *Projected performance of Higgs analyses at the HL-LHC for ECFA 2016*, .
- [98] M. Cepeda et al., *Report from Working Group 2: Higgs Physics at the HL-LHC and HE-LHC*, *CERN Yellow Rep. Monogr.* **7** (2019) 221–584, [[1902.00134](#)].
- [99] C. Englert, F. Krauss, M. Spannowsky and J. Thompson, *Di-Higgs phenomenology in $t\bar{t}hh$: The forgotten channel*, *Phys. Lett. B* **743** (2015) 93–97, [[1409.8074](#)].

- [100] G.-C. Cho, C. Idegawa and E. Senaha, *Electroweak phase transition in a complex singlet extension of the Standard Model with degenerate scalars*, *Phys. Lett. B* **823** (2021) 136787, [[2105.11830](#)].
- [101] L. Niemi, P. Schicho and T. V. I. Tenkanen, *Singlet-assisted electroweak phase transition at two loops*, *Phys. Rev. D* **103** (2021) 115035, [[2103.07467](#)].
- [102] N. F. Bell, M. J. Dolan, L. S. Friedrich, M. J. Ramsey-Musolf and R. R. Volkas, *Two-Step Electroweak Symmetry-Breaking: Theory Meets Experiment*, *JHEP* **05** (2020) 050, [[2001.05335](#)].
- [103] N. F. Bell, M. J. Dolan, L. S. Friedrich, M. J. Ramsey-Musolf and R. R. Volkas, *Electroweak Baryogenesis with Vector-like Leptons and Scalar Singlets*, *JHEP* **09** (2019) 012, [[1903.11255](#)].
- [104] D. E. Ferreira de Lima, A. Papaefstathiou and M. Spannowsky, *Standard model Higgs boson pair production in the $(b\bar{b})(b\bar{b})$ final state*, *JHEP* **08** (2014) 030, [[1404.7139](#)].
- [105] ATLAS collaboration, G. Aad et al., *Search for resonant pair production of Higgs bosons in the $b\bar{b}b\bar{b}$ final state using pp collisions at $\sqrt{s} = 13$ TeV with the ATLAS detector*, [2202.07288](#).
- [106] ATLAS collaboration, G. Aad et al., *Search for the $HH \rightarrow b\bar{b}b\bar{b}$ process via vector-boson fusion production using proton-proton collisions at $\sqrt{s} = 13$ TeV with the ATLAS detector*, *JHEP* **07** (2020) 108, [[2001.05178](#)].
- [107] CMS collaboration, A. M. Sirunyan et al., *Search for nonresonant Higgs boson pair production in the $b\bar{b}b\bar{b}$ final state at $\sqrt{s} = 13$ TeV*, *JHEP* **04** (2019) 112, [[1810.11854](#)].
- [108] CMS collaboration, A. Tumasyan et al., *Search for Higgs boson pair production in the four b quark final state in proton-proton collisions at $\sqrt{s} = 13$ TeV*, [2202.09617](#).
- [109] ATLAS collaboration, G. Aad et al., *Search for resonant and non-resonant Higgs boson pair production in the $b\bar{b}\tau^+\tau^-$ decay channel using 13 TeV pp collision data from the ATLAS detector*, [ATLAS-CONF-2021-030](#).
- [110] ATLAS collaboration, G. Aad et al., *Reconstruction and identification of boosted di- τ systems in a search for Higgs boson pairs using 13 TeV proton-proton collision data in ATLAS*, *JHEP* **11** (2020) 163, [[2007.14811](#)].
- [111] ATLAS collaboration, G. Aad et al., *Combination of searches for non-resonant and resonant Higgs boson pair production in the $b\bar{b}\gamma\gamma$, $b\bar{b}\tau^+\tau^-$ and $b\bar{b}b\bar{b}$ decay channels using pp collisions at $\sqrt{s} = 13$ TeV with the ATLAS detector*, [ATLAS-CONF-2021-052](#).
- [112] CMS collaboration, A. M. Sirunyan et al., *Search for Higgs boson pair production in events with two bottom quarks and two tau leptons in proton-proton collisions at $\sqrt{s} = 13$ TeV*, *Phys. Lett. B* **778** (2018) 101–127, [[1707.02909](#)].
- [113] CMS collaboration, A. M. Sirunyan et al., *Search for Higgs boson pair production in the $b\bar{b}\tau\tau$ final state in proton-proton collisions at $\sqrt{s} = 8$ TeV*, *Phys. Rev. D* **96** (2017) 072004, [[1707.00350](#)].
- [114] CMS collaboration, A. M. Sirunyan et al., *Combination of searches for Higgs boson pair production in proton-proton collisions at $\sqrt{s} = 13$ TeV*, *Phys. Rev. Lett.* **122** (2019) 121803, [[1811.09689](#)].
- [115] F. Arco, S. Heinemeyer and M. J. Herrero, *Triple Higgs Couplings in the 2HDM: The Complete Picture*, [2203.12684](#).